SCIENCE CHINA
Life Sciences

• RESEARCH PAPER •

November 2012 Vol.55 No.11: 968–973
doi: 10.1007/s11427-012-4399-3

Atomic force microscopy imaging and mechanical properties measurement of red blood cells and aggressive cancer cells

LI Mi[1,2,5], LIU LianQing[1*], XI Ning[1,3*], WANG YueChao[1], DONG ZaiLi[1], XIAO XiuBin[4] & ZHANG WeiJing[4*]

[1]*State Key Laboratory of Robotics, Shenyang Institute of Automation, Chinese Academy of Sciences, Shenyang 110016, China;*
[2]*University of Chinese Academy of Sciences, Beijing 100049, China;*
[3]*Department of Mechanical and Biomedical Engineering, City University of Hong Kong, Hong Kong, China;*
[4]*Department of Lymphoma, Affiliated Hospital of Military Medical Academy of Sciences, Beijing 100071, China;*
[5]*State Key Laboratory of Drug Research, Shanghai Institute of Materia Medica, Chinese Academy of Sciences, Shanghai 201203, China*

Received June 4, 2012; accepted October 23, 2012

Mechanical properties play an important role in regulating cellular activities and are critical for unlocking the mysteries of life. Atomic force microscopy (AFM) enables researchers to measure mechanical properties of single living cells under physiological conditions. Here, AFM was used to investigate the topography and mechanical properties of red blood cells (RBCs) and three types of aggressive cancer cells (Burkitt's lymphoma Raji, cutaneous lymphoma Hut, and chronic myeloid leukemia K562). The surface topography of the RBCs and the three cancer cells was mapped with a conventional AFM probe, while mechanical properties were investigated with a micro-sphere glued onto a tip-less cantilever. The diameters of RBCs are significantly smaller than those of the cancer cells, and mechanical measurements indicated that Young's modulus of RBCs is smaller than those of the cancer cells. Aggressive cancer cells have a lower Young's modulus than that of indolent cancer cells, which may improve our understanding of metastasis.

atomic force microscopy, red blood cell, cancer cell, mechanical properties, Young's modulus

Citation: Li M, Liu L Q, Xi N, *et al*. Atomic force microscopy imaging and mechanical properties measurement of red blood cells and aggressive cancer cells. Sci China Life Sci, 2012, 55: 968−973, doi: 10.1007/s11427-012-4399-3

Inside the cell there are many kinds of molecules that interact to form a hierarchical, ordered and active system [1]. Mechanical factors such as hydrostatic pressure, shear stress, tensile forces, and extracellular matrix stiffness crucially regulate cell structure and function [2,3]. Cells adapt dynamically to the stimulation of mechanical forces by modifying their behavior and remodeling their microenvironment [2]; this adaptation is important in embryonic development as well as adult physiology, and is involved in many diseases, including atherosclerosis, hypertension, osteoporosis, muscular dystrophy, and cancer [3]. Cells possess structural and mechanical properties that enable them to both sense mechanical stimuli and to transduce them into regulatory chemical signals [4,5]. Any deviation from these mechano-transduction abilities will influence the biological function of the cell and may potentially result in disease [6]. When normal cells become cancerous, the structure and mechanical properties change [7]. Cross *et al*. [8] reported that cancer cells are more than 70% softer than benign cells. Currently the methods for detecting cancer cells are mainly based on cellular morphology and specific antibody labeling, which can be very complex and not always accurate because normal cells can sometimes look like cancer cells [9]. If changes in mechanical properties during the transfor-

*Corresponding author (email: lqliu@sia.cn; xin@egr.msu.edu; zhangwj3072@163.com)

mation of normal cells to cancer cells can be quantified, new diagnostic methods may emerge [10].

Atomic force microscopy (AFM) [11] provides nanoscale topographic resolution and can dynamically observe changes in mechanical properties of single cells, such as those following stimulation by drugs [12,13]. These aspects have made AFM become an important tool for the measurement of mechanical properties of biomaterials [14,15], and those of cells [16,17]. Cuerrier *et al*. [18] investigated the mechanical properties of human umbilical vein endothelial cells before and after drug treatment. Pelling *et al*. [19] investigated the mechanical properties of human neonatal foreskin fibroblasts during early apoptosis by combining confocal microscopy and AFM. These studies were performed with conventional nanoscale AFM probe tips that are relatively sharp, and thus may cause damage to delicate cells. Moreover, measurements with a conventional probe tip reflect more of the local mechanical properties of the cell, rather than those of the whole cell. In order to circumvent this problem, researchers have attached micro-spheres to a cantilever and used them to measure the mechanical properties of whole cells [20,21]. Here we used homemade sphere probes to measure and compare the mechanical properties of red blood cells and three different aggressive cancer cells. In addition, the topographies of these four cells were mapped with conventional probe tips.

1 Materials and methods

1.1 Principle

The principle of using spherical probes to measure cellular mechanical properties is shown in Fig. 1. Micro-spheres were glued onto tipless AFM cantilevers with epoxy resin. Cells were attached to a glass substrate by coating the substrate with poly-L-lysine (Figure 1A). In the force profile mode, the probe slowly approaches the cell surface, contacts it, and then retracts. By recording the deflection of the cantilever during contact (via a laser beam reflected off the back of the cantilever) and the displacement of the probe driver (piezo tube) during the approach-retract cycle, force profiles are obtained (Figure 1B). When the probe is far away from the cell, the force profile is linear. When the probe contacts the cell, the sphere indents the cell and deflects the cantilever; the force profile thus becomes non-linear and reflects the mechanical properties of the cell. In this way Young's modulus can be determined.

1.2 Sphere probe preparation

CSC12 cantilevers were purchased from MikroMash. The AFM was used to attach the spherical probe (15-μm-diameter polystyrene) as follows: (i) A tipless cantilever was mounted onto the head of the AFM (Dimension 3100, Veeco Company, Santa Barbara, CA, USA) and the laser signal was modulated. (ii) A drop of the polystyrene sphere solution was placed onto a fresh glass slide and a drop of epoxy resin was placed on another section of the same slide. (iii) The AFM controller moved the cantilever to contact the resin and then retracted it. The cantilever was then moved to contact a single sphere and was retracted. The glue was allowed 24 h to harden. The finished probe was imaged with optical microscopy and scanning electron microscopy (SEM), as shown in Figure 1C.

1.3 Cell preparation

Red blood cells (RBCs) from healthy volunteers were diluted in phosphate buffered saline (PBS) and harvested by centrifugation for 10 min at 2000 rpm. Raji/Hut/K562 cells were cultured at 37°C (5% CO_2) in RPMI-1640 containing 10% fetal bovine serum for 24 h before experiments. For imaging, cells were dropped onto glass slides coated with poly-L-lysine and were fixed for 30 min with 4% paraformaldehyde. The glass slide was washed three times with Milli-Q ultra-pure water (18.2 MΩ cm) and dried with a stream of nitrogen. For mechanical measurements, living cells were dropped onto glass slides coated with poly-L-lysine. After one min, the glass slides were placed in a petri dish containing Hank's balanced salt solution (HBSS).

1.4 AFM imaging and measurements

AFM cell imaging experiments were performed in air using

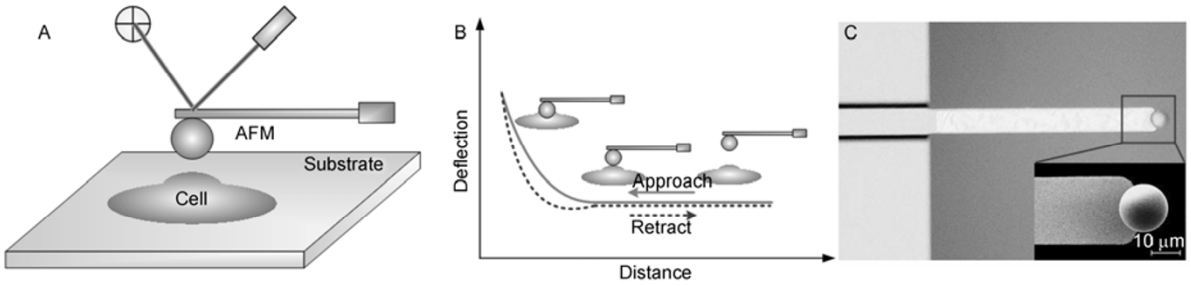

Figure 1 Principle of measuring cellular mechanical properties with a spherical AFM probe. A, Cell is attached onto the substrate, while a sphere is glued onto a tipless cantilever. B, Approach, contact, and retraction to obtain force profiles on the cell surface. C, Optical and SEM images (inset) of a cantilever with a glued sphere.

a conventional probe (MLCT, Veeco Company, Santa Barbara, CA, USA) in contact mode at a scan rate of 1 Hz (256 scan lines and 256 sampling points). The mechanical measurements were performed in HBSS. Force profiles consisted of 512 sampling points and were obtained at a constant loading rate. The cantilever spring constant was calibrated by the thermal tune adapter (Veeco Company, Santa Barbara, CA, USA), and the cantilever sensitivity was calibrated on the bare substrate. Five cells of each type (RBCs, Raji, Hut, K562) were selected and 50 force profiles were obtained on each cell. Young's modulus was computed by applying the Hertz model [21]:

$$F = \frac{4ER^{1/2}\delta^{3/2}}{3(1-\upsilon^2)}, \tag{1}$$

$$\frac{1}{R} = \frac{1}{R_1} + \frac{1}{R_2}, \tag{2}$$

where υ is the Poisson ratio of the cell (0.5), F is the loading force, δ is the indentation depth, E is Young's modulus, R is the effective radius, R_1 is the radius of the sphere, and R_2 is the radius of the cell. The radii of RBCs, Raji, Hut, and K562 cells as measured with an optical microscope are 4, 10, 8, and 12 μm, respectively.

2 Results and discussion

Figure 2 displays AFM images of RBCs, Raji, Hut, and K562 cells. Figure 2A and E shows 12 μm RBC topographic and deflection images, respectively. The unique bi-concave disk shape can be clearly seen. The line profile in Figure 2I indicates a RBC diameter of 7.5 μm. AFM images (40 μm) of a plump, disk-shaped Raji cell are shown in Figure 2B and F. The corresponding line profile reveals a 25 μm diameter. Mature RBCs do not have nuclei and are thus bio-concave disks, while Raji cells are B lymphocytes with nuclei and hence exhibit plump shapes. Hut cells (Figure 2C and G) and K562 cells (Figure 2D and H) are T lymphocytes and neutrophils, respectively. Both have cell nuclei and are circular and plump. From the line profiles, it can be seen that the diameter of the Hut cell is 16 μm (Figure 2K), while the diameter of K562 cell is 28 μm (Figure 2L). The RBC is clearly smaller than the three cancer cells. The normal diameters of healthy human RBCs are 7.5–8.5 μm, diameters of lymphocytes are 6–20 μm, and those of neutrophils are 10–12 μm [22]. Thus the RBC diameter in Figure 2 is normal. The diameter of the Hut cell is a normal cell size as well. However, the Raji and K562 cells are significantly larger than normal healthy cells. The RBCs were

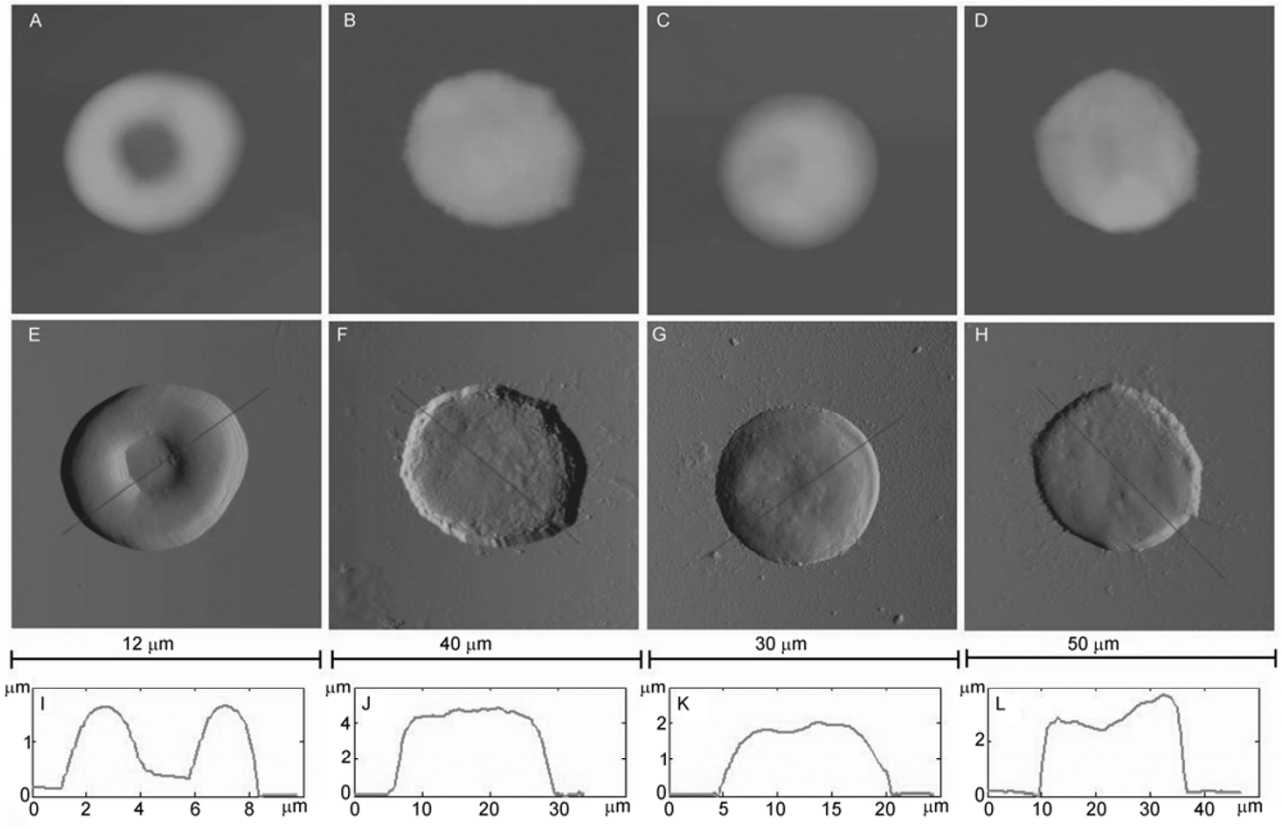

Figure 2 AFM images of RBC, Raji, Hut, and K562 cells. A, Topography of a RBC. B, A Raji cell. C, A Hut cell. D, A K562 cell. E, Deflection image of RBC. F, Deflection image of Raji cell. G, Deflection image of Hut cell. H, Deflection image of K562 cell. I, Line profile of RBC. J, Line profile of Raji cell. K, Line profile of Hut cell. L, Line profile of K562 cell.

from healthy volunteers, while the others are cancer cells that are often larger than healthy cells.

After obtaining force profiles with a spherical probe on the surfaces of several RBCs, Young's modulus was computed as shown in Figure 3. Figure 3A is a typical force profile consisting of both approach (black) and retract (red) data. There is a gap (hysteresis) between the approach and retract profiles that is caused by cellular viscosity. The cell is viscoelastic, i.e., it has a viscosity of fluids and an elasticity of solids [23]. The small gap indicates that during the approach-retract process, the viscosity of the cell was small and the elasticity was dominant. This is a consistent characteristic of RBCs since they have high elasticity. Biomembrane force probe technology is based on this high elasticity [24]. The approach profile was converted into an indentation profile following the point of contact. The 500 nm range of the indentation profile was used to compute Young's modulus. For each force profile, several hundred values of Young's modulus were computed [25], and a histogram was plotted (Figure 3C). Insertion of Young's modulus (Gaussian fit: 0.173 kPa) into the Hertz model formula produced a theoretical indentation curve that is compared with the experimental data in Figure 3D. The good agreement indicates that the Hertz model is an adequate approximation of the sphere indentation process [26]. For each RBC, 50 force curves were obtained and 50 values of Young's modulus were computed; a histogram is shown in Figure 3E. A Gaussian fit indicates that Young's modulus of the RBC was (0.143±0.059) kPa. Values of Young's modulus for four other RBCs were (0.137±0.060), (0.149±0.1), (0.146±0.027), and (0.143±0.07) kPa. Figure 3F is the histogram of Young's modulus of all RBCs.

By applying the same procedure described above, Young's modulus values for Raji, Hut, and K562 cells were computed and the results are shown in Figure 4. Young's modulus of Raji cells is 0.2–0.4 kPa, that of Hut cells is 1–1.4 kPa, and that of K562 cells is 0.6–0.7 kPa. Comparing the results for the Raji cells to previous values obtained with a conventional probe ((150±60) kPa) [25,26], we can see that Young's modulus measured with a spherical probe (0.2–0.4 kPa) is significantly smaller. This difference is most likely a result of the spherical probe measuring the mechanical properties of the whole cell, while the conventional probe measured those in a local area of the cell. Since the cell is heterogeneous, mechanical properties will vary widely between local areas and the whole cell. Young's modulus previously measured with a spherical probe is 0.2–1.2 kPa for breast cancer cells [21,27], and is 0.5 kPa for macrophages [28]. Thus the 0.1–1.4 kPa values presented here for Young's modulus of RBCs, Raji, Hut, and K562 cells are comparable to those published previously.

The order of increasing Young's modulus is RBCs (smallest), followed by Raji, K562, and Hut cells (largest). The special nucleus-free structure of RBCs (Figure 5A) may result in the small Young's modulus. The softness of an RBC makes it easy to deform, and allows it to traverse narrow capillaries [22] and carry oxygen to various parts of the body. On the basis of Young's modulus for Raji and Hut cells, the latter are much stiffer. The Raji cells were from Burkitt's lymphoma that is an aggressive, malignant B-cell

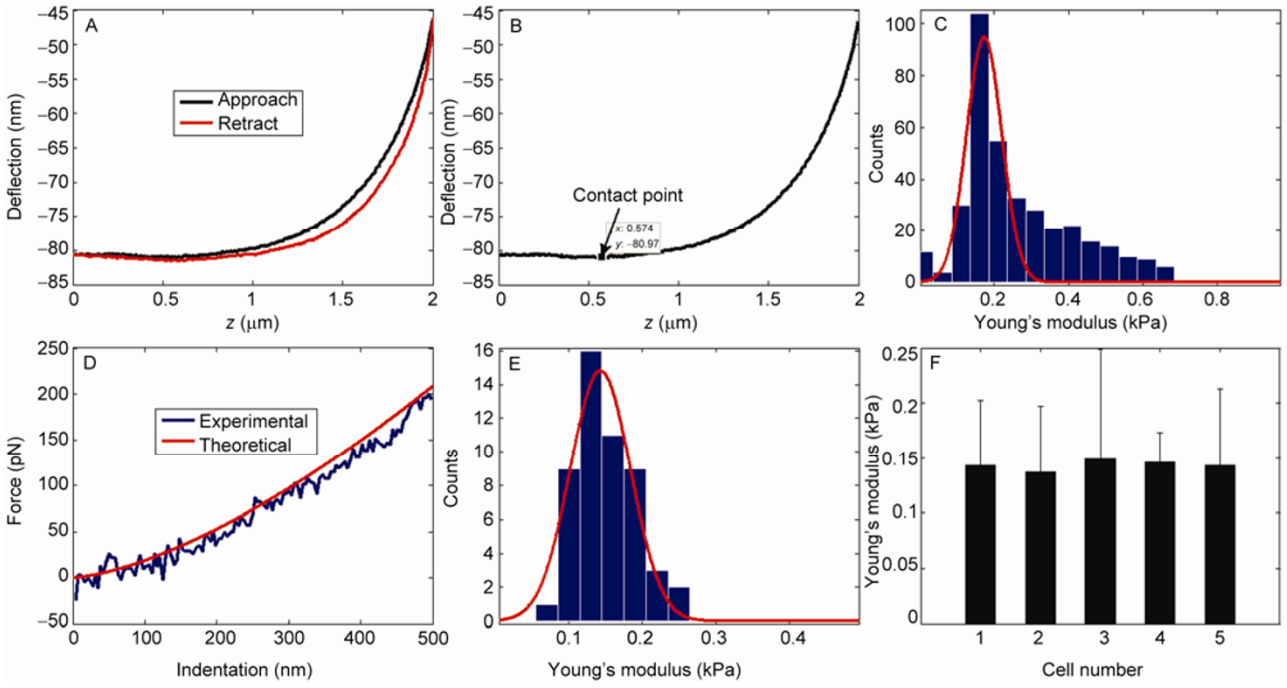

Figure 3 Obtaining Young's modulus for RBCs. A, A typical force profile. B, Approach portion of force profile. C, Histogram of Young's modulus from approach profiles and Gaussian fit (red). D, Comparison of experimental (blue) and theoretical (red) indention profiles. E, Histogram of Young's modulus for one cell and Gaussian fit (red). F, Histogram of Young's modulus for five RBCs.

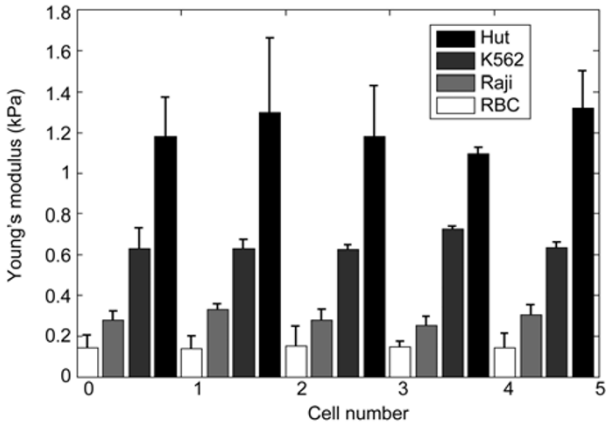

Figure 4 Histogram of Young's modulus for RBCs, Raji, Hut, and K562 cells.

lymphoma characterized by a high degree proliferation [29]. The Hut cells were from Sezary syndrome, which is a cutaneous T-cell lymphoma characterized by indolent malignant cells [30]. We can see here that the Raji cells were soft, while Hut cells were stiff. K562 cells were from chronic myeloid leukemia [31]. These cancer cells are also indolent, and we see that the Young's modulus is larger than that of the Raji cells.

In the process of metastasis from a primary site to a distant site, cancer cells must first pass through the basement membrane, then they pass through the extracellular matrix, and finally they penetrate the blood vessel walls [32]. As is shown schematically in Figure 5B, the blood flow helps them to move to other tissues and organs where they settle and proliferate. Jin *et al.* [33] measured the mechanical properties of breast cancer cells after treatment with bone morphogenetic protein (BMP) that promotes cell migration; the results indicated that after BMP stimulation, the cells became softer. Cross *et al*. [8] indicated that cancer cells were much softer than normal cells. These results thus indicate that softness is important for cell migration and that it may make it easier for cancer cells to cross various obstacles in the body. Various cancer cells have different metastatic capabilities; some are indolent, whereas some are aggressive. This difference may be related to the ability to cross obstacles that, in turn, is related to cell softness. For the three cancer cells investigated here, Raji cells are the most aggressive and the softest, while the Hut and K562 cells are indolent and stiffer. Cell mechanical properties are closely related to their structures [1], such as membranes or the cytoskeleton, and thus can be quite variable. Here, we measured the mechanical properties of three different cancer cells having different levels of aggressiveness. The results indicated that aggressive cancer cells are softer than indolent cancer cells, providing a possible insight into metastasis. However, the underlying structures that cause these differences are unknown and require further research.

3 Conclusion

With the widespread application of AFM in cell biology, new knowledge has been acquired concerning the relationship between mechanical properties and diseases. Using homemade spherical probes, we quantitatively investigated the mechanical properties of RBCs, Raji, Hut, and K562 cells. The results indicate that Young's modulus of RBCs is 0.1–0.2 kPa, that of Raji cells is 0.2–0.4 kPa, that of Hut cells is 1–1.4 kPa, and that of K562 cells is 0.6–0.7 kPa. These results indicate that aggressive cancer cells are softer than indolent cells, and thus possibly better able to migrate.

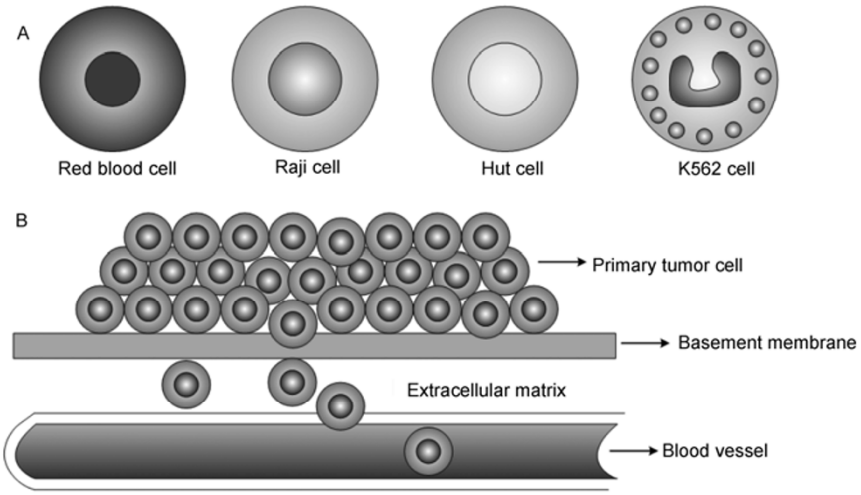

Figure 5 Cellular mechanical properties and cancer metastasis. A, Structure of RBC, Raji, Hut, K562 cells. B, Schematic of cancer cell metastasis.

This work was supported by the National Natural Science Foundation of China (Grant Nos. 60904095 and 61175103), CAS FEA International Partnership Program for Creative Research Teams and the State Key Laboratory of Drug Research.

1 Fletcher D A, Mullins R D. Cell mechanics and the cytoskeleton. Nature, 2010, 463: 485–492
2 Butcher D T, Alliston T, Weaver V M. A tense situation: forcing tumor progression. Nat Rev Cancer, 2009, 9: 108–122
3 Hoffman B D, Grashoff C, Schwartz M A. Dynamic molecular processes mediate cellular mechanotransduction. Nature, 2011, 475: 316–323
4 Janmey P A, McCulloch C A. Cell mechanics: integrating cell responses to mechanical stimuli. Annu Rev Biomed Eng, 2007, 9: 1–34
5 Lim C T, Zhou E H, Quek S T. Mechanical models for living cells—a review. J Biomech, 2006, 39: 195–216
6 Li Q S, Lee G Y H, Ong C N, *et al*. AFM indentation study of breast cancer cells. Biochem Biophys Res Commun, 2008, 374: 609–613
7 Suresh S. Biomechanics and biophysics of cancer cells. Acta Biomater, 2007, 3: 413–438
8 Cross S E, Jin Y S, Rao J Y, *et al*. Nanomechanical analysis of cells from cancer patients. Nat Nanotechnol, 2007, 2: 780–783
9 Suresh S. Elastic clues in cancer detection. Nat Nanotechnol, 2007, 2: 748–749
10 Yu H, Mouw J K, Weaver V M. Forcing form and function: biomechanical regulation of tumor evolution. Trends Cell Biol, 2011, 21: 47–56
11 Binning G, Quate C F, Gerber C. Atomic force microscope. Phys Rev Lett, 1986, 56: 930–933
12 Martens J C, Radmacher M. Softening of the actin cytoskeleton by inhibition of myosin II. Pflugers Arch Eur J Physiol, 2008, 456: 95–100
13 Li M, Liu L, Xi N, *et al*. Imaging and measuring the rituximab-induced changes of mechanical properties in B-lymphoma cells using atomic force microscopy. Biochem Biophys Res Commun, 2011, 404: 689–694
14 Tao N J, Lindsay S M, Lees S. Measuring the microelastic properties of biological material. Biophys J, 1992, 63: 1165–1169
15 Radmacher M, Monika F, Hansma P K. Imaging soft samples with the atomic force microscope: gelatin in water and propanol. Biophys J, 1995, 69: 264–270
16 Hoh J H, Schoenenberger C A. Surface morphology and mechanical properties of MDCK monolayers by atomic force microscopy. J Cell Sci, 1994, 107: 1105–1114
17 Radmacher M, Fritz M, Kacher C M, *et al*. Measuring the viscoelastic properties of human platelets with the atomic force microscope. Biophys J, 1996, 79: 556–567
18 Cuerrier C M, Gagner A, Lebel R, *et al*. Effect of thrombin and bradykinin on endothelial cell mechanical properties monitored through membrane deformation. J Mol Recognit, 2009, 22: 389–396
19 Pelling A E, Veraitch F S, Chu C P K, *et al*. Mechanical dynamics of single cells during early apoptosis. Cell Motil Cytoskeleton, 2009, 66: 409–422
20 Oberleithner H, Callies C, Kusche-Vihrog K, *et al*. Potassium softens vascular endothelium and increases nitric oxide release. Proc Natl Acad Sci USA, 2009, 106: 2829–2834
21 Nikkhah M, Strobl J S, Schmelz E M, *et al*. Evaluation of the influence of growth medium composition on cell elasticity. J Biomech, 2011, 44: 762–766
22 Gao Y M, Xu C F. Histology and Embryology (in Chinese). Beijing: People's Medical Publishing House, 2001. 64–65
23 Butt H J, Cappella B, Kappl M. Force measurements with the atomic force microscope: technique, interpretation and applications. Surf Sci Rep, 2005, 59: 1–152
24 Merkel R, Nassoy P, Leung A, *et al*. Energy landscapes of receptor-ligand bonds explored with dynamic force spectroscopy. Nature, 1999, 397: 50–53
25 Li M, Liu L Q, Xi N, *et al*. Imaging and mechanical property measurement of the lymphoma cells by atomic force microscopy (in Chinese). Chin Sci Bull, 2010, 55: 2188–2196
26 Li M, Liu L, Xi N, *et al*. Drug-induced changes of topography and elasticity in living B lymphoma cells based on atomic force microscopy. Acta Phys Chim Sin, 2012, 28: 1502–1508
27 Nikkhah M, Strobl J S, Vita R D, *et al*. The cytoskeletal organization of breast carcinoma and fibroblast cells inside three dimensional (3-D) isotropic silicon microstructures. Biomaterials, 2010, 31: 4552–4561
28 Leporatti S, Gerth A, Kohler G, *et al*. Elasticity and adhesion of resting and lipoplysaccharide-stimulated macrophages. FEBS Lett, 2006, 580: 450–454
29 Dave S S, Fu K, Wright G W, *et al*. Molecular diagnosis of Burkitt's lymphoma. N Engl J Med, 2006, 354: 2431–2442
30 Diamandidou E, Cohen P R, Kurzrock R. Mycosis fungoides and sezary syndrome. Blood, 1996, 88: 2385–2409
31 Deininger M W N, Goldman J M, Melo J V. The molecular biology of chronic myeloid leukemia. Blood, 2000, 96: 3343-3356
32 Lee G Y H, Lim C T. Biomechanics approaches to studying human diseases. Trends Biotechnol, 2007, 25: 111–118
33 Jin H, Pi J, Huang X, *et al*. BMP2 promotes migration and invasion of breast cancer cells via cytoskeletal reorganization and adhesion decrease: an AFM investigation. Appl Microbiol Biotechnol, 2012, 93: 1715–1723